Journal of Sound and Vibration (2000) **235**(3), 415–434
doi:10.1006/jsvi.2000.2930, available online at http://www.idealibrary.com on IDEAL®

ANALYTICAL APPROACH TO THE DETERMINATION OF DYNAMIC CHARACTERISTICS OF A BEAM WITH A CLOSING CRACK

A. P. Bovsunovsky and V. V. Matveev

Department of Oscillations and Vibration Reliability, Institute for Problems of Strength, National Academy of Sciences of Ukraine, Timiryazevskaya st.2, Kyiv 252014, *Ukraine*

(*Received* 24 *September* 1999, *and in final form* 14 *December* 1999)

A wide spectrum of investigations devoted to the determination of natural frequencies and mode shapes of beams with an open crack are presented in the literature. However, as is well known, an open crack is a fairly crude model of a fatigue crack. The study of the dynamic characteristics of a beam with a closing crack is the main aim of the present paper. The analytical approach which enables one to determine the effect of crack parameters (crack magnitude and location) on different dynamic characteristics of a cantilever Bernoulli–Euler beam with a closing edge transverse crack is performed. Natural frequencies, mode shapes and distortion of time functions describing wave shapes of displacement, acceleration and strain of different cross-sections of a beam are considered as dynamic characteristics to be investigated. The general solution of the problem is derived from the synthesis of particular solutions obtained for the crack-free beam and for the beam with an open crack. The possibility of origination of several modes of vibrations during crack opening is taken into account as well as the peculiarity of strain distribution in the vicinity of a crack. It is shown that analytically predicted relationships between the dynamic characteristics of a cracked beam and crack parameters are well-founded. The analytical approach makes it possible to solve the inverse problem of damage diagnostics with sufficient accuracy for practical purposes.

1. INTRODUCTION

Dynamic characteristics of a damaged and undamaged body are, as a rule, different. This difference is caused by a change in stiffness and can be used for the detection of damage and for the determination of its parameters (crack magnitude and location).

It follows from the Krawczuk and Ostachowicz [1] survey of works dedicated to the determination of relationships between vibration damage characteristics and crack parameters that most studies attempt to employ the natural frequency of vibration as a damage characteristic. However, it should be noted that the results of other experimental and analytical investigations of the eigenfrequency problem [2–11], mode shapes [12, 13] or mode shapes and natural frequencies [14–16] of a cracked body were not reflected in the survey [1]. In references [1–16] with the exception of references [5, 11] the so-called open crack was considered. As is well known, an open crack is a crude model of fatigue crack: the latter must be considered rather as a closing ("breathing") one. This assumption is confirmed by the results of an experiment reported by Gudmundson [4] who established that the measured drop in natural frequency of the specimen with a fatigue crack was considerably less than that predicted theoretically for the beam with an open crack.

0022-460X/00/330415 + 20 $35.00/0

The results of investigations [17–22] of vibrations of mechanical system, modelling the body with a closing crack, show that the distortion of wave shapes of different vibration characteristics is a promising way for diagnostics of fatigue cracks. The distortion of a wave shape was judged by the presence of higher harmonics in the Fourier-series expansion of the corresponding time function. In the present paper, this vibration damage characteristic is examined, as applied to a cracked beam, in parallel with the natural frequencies and mode shapes.

The accuracy of analytical determination of vibration characteristics of a cracked body depends mainly on the crack model. A wide spectrum of such models can be found in the literature: a crack was modelled by a spring [5, 23], elastic hinge [8, 12], cut-out [14], a pair of concentrated couples [15, 24], a zone with reduced Young's modulus [7, 23], or its effect was taken into account by semi-empirical functions describing stress and strain distribution by the volume of cracked beam [16, 25]. Chati *et al.* [26] modelled the process of crack opening and closing by means of a piecewise-linear system. The approach to crack modelling presented here is based on the assumption that the beam is of constant cross-section along the length, and the crack is modelled by a zone with reduced moment of inertia. The dimensions of this zone are determined from energy criteria [8]. It is presumed that such a crack model is physically justified inasmuch as the decrease in moment of inertia and the shift of the neutral axis in the cross-section with a crack in fact take place.

Petroski [24] inferred that the vibration response of a cracked beam to a suddenly applied and held load demonstrates the effect of the crack in introducing the higher frequency vibrations more noticeably into the total response. This signifies that the process of crack opening or closing is the additional cause of the higher mode shapes that appear under vibrations of the cracked beam and must be taken into account.

The purpose of the present paper is to develop the analytical approach enabling the simulation of vibration of a beam with a closing edge transverse crack in order to solve direct (determination of dynamic characteristics of a beam at given crack parameters) and inverse (estimation of crack parameters by the known values of corresponding dynamic characteristics) problems of damage diagnostics. The natural frequencies and mode shapes of a beam and distortion of the displacement, acceleration and strain wave shapes were chosen as the dynamic characteristics to be investigated.

2. DYNAMIC CHARACTERISTICS OF A BEAM WITH AN OPEN CRACK

Let us consider a cantilever beam of constant rectangular cross-section with a mass on the end. It is well known that the free bending vibrations of such a beam with the damping effect neglected are described by the differential equation

$$\frac{\partial^4 y(x,t)}{\partial x^4} + \frac{\rho A}{EI}\frac{\partial^2 y(x,t)}{\partial t^2} = 0, \tag{1}$$

where E and ρ are Young's modulus and density of the beam material, respectively, $I = bh^3/12$ and $A = bh$ are the moment of inertia and area of the cross-section, respectively, and b and h are the width and height of cross-section respectively.

The general solution of equation (1) can be presented in a following form:

$$y(x,t) = \sum_{i=1}^{\infty} w_i(x)(P_i \sin \omega_i t + R_i \cos \omega_i t), \tag{2}$$

where $w_i(x)$ and ω_i are the mode shapes and natural angular velocities, respectively, and i is the number of the mode shape. The mode shapes of the beam are described by the expression

$$w_i(x) = A_i S(k_i x) + B_i T(k_i x) + C_i U(k_i x) + D_i V(k_i x), \tag{3}$$

where $k_i^4 = \omega_i^2 \rho A/EI$, $S(k_i x) = (\cosh k_i x + \cos k_i x)/2$, $T(k_i x) = (\sinh k_i x + \sin k_i x)/2$, $U(k_i x) = (\cosh k_i x - \cos k_i x)/2$, $V(k_i x) = (\sinh k_i x - \sin k_i x)/2$ (S, T, U, V are the Krylov functions).

The coefficients A_i, B_i, C_i and D_i in expression (3) are determined from the boundary conditions

$$w_i(0) = 0, \qquad \theta_i(0) = \frac{\partial w_i(0)}{\partial x} = 0, \qquad M_i(L) = EI \frac{\partial^2 w_i(L)}{\partial x^2} = I_m \omega_i^2 \frac{\partial w_i(L)}{\partial x},$$

$$Q_i(L) = EI \frac{\partial^3 w_i(L)}{\partial x^3} = -m_L \omega_i^2 w_i(L), \tag{4}$$

where θ is the angle of rotation of the cross-section, M is the bending moment, Q is the transverse force, L is the length of the beam, m_L is the mass on the end, and I_m is the moment of inertia of the mass.

The characteristic equation in this case assumes the form

$$[S(k_i L) - qT(k_i L)][S(k_i L) + gV(k_i L)] - [T(k_i L) - qU(k_i L)][V(k_i L) + gU(k_i L)] = 0, \tag{5}$$

where $q = I_m k_i^3/\rho A$, $g = m_L k_i/\rho A$.

Taking coefficient C_i to be $C_i = M(0)/EIk_i^2$ one can obtain

$$w_i(x) = \frac{M(0)}{EIk_i^2}\left[U(k_i x) - \frac{V(k_i L) + gU(k_i L)}{S(k_i L) + gV(k_i L)} V(k_i x)\right]. \tag{6}$$

The coefficients P_i and R_i in equation (2) are determined by the formulae [27]

$$P_i = \frac{\omega_i F_1 \sin \omega_i t_1 + F_2 \cos \omega_i t_1}{\omega_i \left[\int_0^L m w_i^2(x)\,\mathrm{d}x + m_L w_i^2(L) + I_m \theta_i^2(L)\right]}, \tag{7}$$

$$R_i = \frac{\omega_i F_1 \cos \omega_i t_1 - F_2 \sin \omega_i t_1}{\omega_i \left[\int_0^L m w_i^2(x)\,\mathrm{d}x + m_L w_i^2(L) + I_m \theta_i^2(L)\right]}, \tag{8}$$

where $m = \rho A$ is the beam mass per unit length,

$$F_1 = \int_0^L m y_1(x) w_i(x)\,\mathrm{d}x + m_L y_1(L) w_i(L) + I_m \theta_1(L) \theta_i(L),$$

$$F_2 = \int_0^L m v_1(x) w_i(x)\,\mathrm{d}x + m_L v_1(L) w_i(L) + I_m \left[\frac{\partial \theta(L, t)}{\partial t}\right]_{t=t_1} \theta_i(L),$$

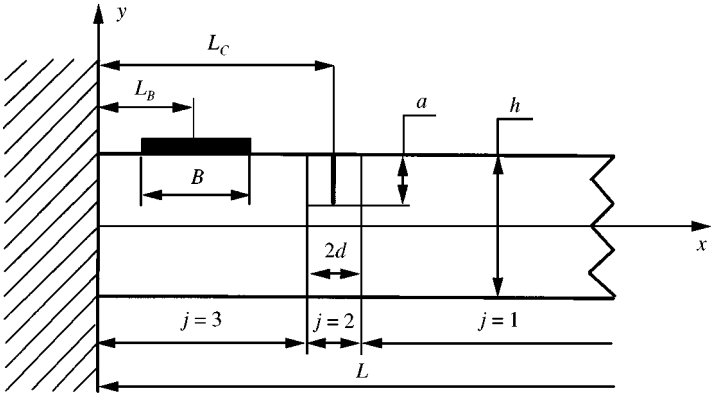

Figure 1. Geometry of cracked cantilever beam (B is the base of strain guage).

from the initial conditions for the displacement, velocity and angle of rotation, respectively, at certain instant of time t_1:

$$y(x, t_1) = y_1(x), \qquad \left[\frac{\partial y(x, t)}{\partial t}\right]_{t=t_1} = v_1(x), \qquad \theta(x, t_1) = \theta_1(x).$$

Let us consider a beam equivalent to one with an open edge transverse crack (such a crack is supposed to be open on both half-cycles of vibration) located at a distance L_c from the clamped end (Figure 1). In this equivalent beam, the crack is modelled by the short section with reduced moment of inertia of the cross-section (section $j = 2$ in Figure 1). The dimension of this section 2d is varied, based on the energy criterion the essence of which is described below. At the same time, the cross-section area of the beam was supposed to be constant. In such a manner the inertia characteristic of the beam remains unchanged.

Free bending vibrations of each section of the equivalent beam with the damping effect neglected are described by the differential equation (1) in which $I = I_j$ is the cross-sectional moment of inertia of the section number j ($j = 1, 2, 3$), $I_1 = I_3 = I$; $I_2 = I_o = b(h - a)^3/12$, and a is the crack depth (subscript "o" signifies the open crack).

In this case, the general solution of equation (1) for the section number j takes the form

$$y_{oj}(x, t) = \sum_{i=1}^{\infty} w_{ij}(x)(P_{oi} \sin \omega_{oi} t + R_{oi} \cos \omega_{oi} t) \tag{9}$$

Expressions for the mode shapes of the equivalent beam must be written for each section as

$$w_{ij}(x) = A_{ij} S(k_{ij} x) + B_{ij} T(k_{ij} x) + C_{ij} U(k_{ij} x) + D_{ij} V(k_{ij} x), \tag{10}$$

where $k_{ij}^4 = \omega_{oi}^2 \rho A / E I_j$, and ω_{oi} is the natural angular velocity of a beam with an open crack. From expression (10), the functions can be derived to describe the angle of rotation $\theta_{ij}(x)$, bending moment $M_{ij}(x)$ and transverse force $Q_{ij}(x)$ as

$$\theta_{ij}(x) = k_{ij}[A_{ij} V(k_{ij} x) + B_{ij} S(k_{ij} x) + C_{ij} T(k_{ij} x) + D_{ij} U(k_{ij} x)], \tag{11}$$

$$M_{ij}(x) = E I_j k_{ij}^2 [A_{ij} U(k_{ij} x) + B_{ij} V(k_{ij} x) + C_{ij} S(k_{ij} x) + D_{ij} T(k_{ij} x)], \tag{12}$$

$$Q_{ij}(x) = E I_j k_{ij}^3 [A_{ij} T(k_{ij} x) + B_{ij} U(k_{ij} x) + C_{ij} V(k_{ij} x) + D_{ij} S(k_{ij} x)]. \tag{13}$$

Boundary conditions and conditions of compatibility on the boundaries of section $j = 2$ for the equivalent beam with the end mass will appear as

$$M_{i1}(L) = I_m\omega_{oi}^2 k_{i1}[A_{i1}V(k_{i1}L) + B_{i1}S(k_{i1}L) + C_{i1}T(k_{i1}L) + D_{i1}U(k_{i1}L)],$$

$$Q_{i1}(L) = -m\omega_{oi}^2[A_{i1}S(k_{i1}L) + B_{i1}T(k_{i1}L) + C_{i1}U(k_{i1}L) + D_{i1}V(k_{i1}L)],$$

$$w_{i1}(x_2) = w_{i2}(x_2), \quad \theta_{i1}(x_2) = \theta_{i2}(x_2), \quad M_{i1}(x_2) = M_{i2}(x_2), \quad Q_{i1}(x_2) = Q_{i2}(x_2),$$

$$w_{i2}(x_1) = w_{i3}(x_1), \quad \theta_{i2}(x_1) = \theta_{i3}(x_1), \quad M_{i2}(x_1) = M_{i3}(x_1), \quad Q_{i2}(x_1) = Q_{i3}(x_1),$$

$$w_{i3}(0) = 0, \quad \theta_{i3}(0) = 0,$$

where $x_1 = L_c - d$, $x_2 = L_c + d$.

Taking into consideration the properties of the Krylov functions ($S(0) = 1$; $T(0) = U(0) = V(0) = 0$) and the two last boundary conditions one finds that $A_{i3} = B_{i3} = 0$. Residuary boundary and compatibility conditions determine the set of equations the determinant of which takes the form

$$\begin{vmatrix}
a_{11} & a_{12} & a_{13} & a_{14} & 0 & 0 & 0 & 0 & 0 & 0 \\
a_{21} & a_{22} & a_{23} & a_{24} & 0 & 0 & 0 & 0 & 0 & 0 \\
-S(\delta) & -T(\delta) & -U(\delta) & -V(\delta) & S(\chi) & T(\chi) & U(\chi) & V(\chi) & 0 & 0 \\
-V(\delta) & -S(\delta) & -T(\delta) & -U(\delta) & r_1V(\chi) & r_1S(\chi) & r_1T(\chi) & r_1U(\chi) & 0 & 0 \\
-U(\delta) & -V(\delta) & -S(\delta) & -T(\delta) & r_2U(\chi) & r_2V(\chi) & r_2S(\chi) & r_2T(\chi) & 0 & 0 \\
-T(\delta) & -U(\delta) & -V(\delta) & -S(\delta) & r_1^{-1}T(\chi) & r_1^{-1}U(\chi) & r_1^{-1}V(\chi) & r_1^{-1}S(\chi) & 0 & 0 \\
0 & 0 & 0 & 0 & -S(\xi) & -T(\xi) & -U(\xi) & -V(\eta) & V(\eta) & U(\eta) \\
0 & 0 & 0 & 0 & -V(\xi) & -S(\xi) & -T(\xi) & -U(\eta) & r_1^{-1}U(\eta) & r_1^{-1}T(\eta) \\
0 & 0 & 0 & 0 & -U(\xi) & -V(\xi) & -S(\xi) & -T(\eta) & r_2^{-1}T(\eta) & r_2^{-1}S(\eta) \\
0 & 0 & 0 & 0 & -T(\xi) & -U(\xi) & -V(\xi) & -S(\eta) & r_1S(\eta) & r_1V(\eta)
\end{vmatrix} = 0, \tag{14}$$

where $a_{11} = U(\varphi_i) - q_oV(\varphi_i)$, $a_{12} = V(\varphi_i) - q_oS(\varphi_i)$, $a_{13} = S(\varphi_i) - q_oT(\varphi_i)$, $a_{14} = T(\varphi_i) - q_oU(\varphi_i)$, $a_{21} = T(\varphi_i) + g_oS(\varphi_i)$, $a_{22} = U(\varphi_i) + g_oT(\varphi_i)$, $a_{23} = V(\varphi_i) + g_oU(\varphi_i)$, $a_{24} = S(\varphi_i) + g_oV(\varphi_i)$, $\varphi_i = k_{i1}L$, $\delta_i = k_{i1}x_2 = x_2\varphi_i/L$, $\chi_i = k_{i2}x_2 = x_2r_1\varphi_i/L$, $\xi_i = k_{i2}x_1 = x_1r_1\varphi_i/L$, $\eta_i = k_{i3}x_1 = x_1\varphi_i/L$, $r_1 = r^{-0,25}$, $r_2 = r^{0,5}$, $r = I_o/I$, $q_o = I_m\varphi_i^3/\rho AL^3$, $g_o = m_L\varphi_i/\rho AL$.

The solution of characteristic equation (14) enables one to calculate the natural frequencies of the beam with an open crack:

$$\omega_{oi} = \frac{\varphi_i^2}{L^2}\sqrt{\frac{EI}{\rho A}}. \tag{15}$$

When solving the set of equations by the Gauss method the coefficient C_{i3} is taken to be the same as in the case of the crack-free beam and in doing so $M_{i3}(0) = M(0)$. It is also assumed that on the boundaries of the section $j = 2$, the cross-sectional moment of inertia is equal to I.

The reduction of the cross-sectional moment of inertia causes the change in strain energy. The change in strain energy of the section $j = 2$ of the equivalent beam, if the change in

bending moment $M(x)$ along the beam length is neglected, is equal to

$$\Delta U_2 = \frac{12M^2 d}{bh^3 E}\left[1 - \frac{1}{(1-\gamma)^3}\right], \tag{16}$$

where $\gamma = a/h$. In the linearly elastic body the change of strain energy due to crack presence of the mode I deformation in the assumption of plane stress will be as follows [28]:

$$\Delta U = \frac{b}{E}\int_0^a K_I^2 \, \mathrm{d}a. \tag{17}$$

Here the expression for the stress intensity factor obtained by Cherepanov for the case of pure bending of a cracked strip [29] is used:

$$K_I = \frac{4{\cdot}2M}{bh^{3/2}}\left[(1-\gamma)^{-3} - (1-\gamma)^3\right]^{1/2}. \tag{18}$$

Inasmuch as in the frequency range being investigated the strain wavelength is greater by several orders of magnitude than the crack size, the elastic field in its neighborhood can be considered as quasi-static [29]. This makes it possible to neglect the influence of the dynamic effect on the stress intensity factor. Substitution of equation (18) into equation (17) gives

$$\Delta U = \frac{4{\cdot}41M^2}{bh^2 E}(1-\gamma)^{-2}\left[(1-\gamma)^6 - 3(1-\gamma)^2 + 2\right]. \tag{19}$$

The energy criterion for equivalence of the cracked beam and its model has the appearance

$$\Delta U_2 = \Delta U. \tag{20}$$

From equation (20) and equations (16) and (19) the parameter d is derived as

$$d = \frac{0{\cdot}3675h(1-\gamma)}{1-(1-\gamma)^3}\left[(1-\gamma)^6 - 3(1-\gamma)^2 + 2\right]. \tag{21}$$

3. DYNAMIC CHARACTERISTICS OF A BEAM WITH A CLOSING CRACK

Consider now a beam with the so-called closing crack; such a crack is supposed to be open on the half-cycle of vibration and closed on another one. Suppose that at certain initial instant of time $t_1 = -\pi/2\omega_s$ the crack is closed and that a beam with a closed crack does not differ from the crack-free beam. Then the displacement of the beam cross-sections and their velocities are determined by the expressions

$$y_1(x) = w_s(x), \qquad v_1(x) = 0 \tag{22}$$

(subscript "s" signifies the initial mode shape). With the condition of mode shapes orthogonality

$$\int_0^L m w_s(x) w_i(x)\,\mathrm{d}x + m_L w_s(L) w_i(L) + I_m \theta_s(L)\theta_i(L) = 0 \tag{23}$$

($s \neq i$), and from equations (7) and (8) it is found that $P_s = 1$, $P_{i \neq s} = R_i = 0$. In doing so, equation (2) simplifies to the form

$$y(x, t) = w_s(x) \sin \omega_s t. \tag{24}$$

On the other half-cycle, while the crack is open, the equation of vibration takes the form similar to equation (9):

$$y_{cj}(x, t) = \sum_{i=1}^{\infty} w_{ij}(x)(P_{ci} \sin \omega_{oi} t + R_{ci} \cos \omega_{oi} t) \tag{25}$$

(subscript "c" signifies the closing crack). It is assumed that the crack begin to open at the instance of time $t_2 = 0$; that is when the beam passes through the neutral position. Then, from equation (24), one can obtain the initial conditions for the beam with closing crack at the instant of crack opening

$$y_1(x) = 0, \qquad v_1(x) = \omega_s w_s(x). \tag{26}$$

With equations (7) and (8), and using equation (26), it is not difficult to show that $R_{ci} = 0$ and

$$P_{ci} = \frac{\omega_s}{\omega_{oi}} \frac{\int_0^{L_c - d} m w_s(x) w_{i3}(x)\,\mathrm{d}x + \int_{L_c - d}^{L_c + d} m w_s(x) w_{i2}(x)\,\mathrm{d}x + \int_{L_c + d}^{L} m w_s(x) w_{i1}(x)\,\mathrm{d}x + F_3}{\int_0^{L_c - d} m w_{i3}^2(x)\,\mathrm{d}x + \int_{L_c - d}^{L_c + d} m w_{i2}^2(x)\,\mathrm{d}x + \int_{L_c + d}^{L} m w_{i1}^2(x)\,\mathrm{d}x + F_4}, \tag{27}$$

where $F_3 = m_L w_s(L) w_{i1}(L) + I_m \theta_s(L) \theta_{i1}(L)$, $F_4 = m_L w_{i1}^2(L) + I_m \theta_{i1}^2(L)$.

Equation (25) is simplified to the form

$$y_{cj}(x, t) = P_{cs} w_{sj}(x) \sin \omega_{os} t + \sum_{i \neq s}^{\infty} P_{ci} w_{ij}(x) \sin \omega_{oi} t. \tag{28}$$

Equations (24) and (28) determine the solution for the first cycle of vibration. In a similar way, one can deduce the solution for the second and subsequent cycles. The initial conditions for the beam at the instant of crack closing are derived from equation (28) and at the instant of crack opening from equation (2). In the general case, each cycle of vibration will be described by its own pair of equations (2) and (25). However, this way of solving the problem discussed is not considered within the framework of the present paper.

This analysis is restricted to the first cycle of vibration. As can be seen from equation (28) the crack opening may generate the concomitant ($i \neq s$) mode shapes. The values of coefficients P_{ci} for different specimens (see Table 1) were calculated with the use of equation (27) in cases $s = 1$ and 2. As can be seen from Figure 2, the amplitudes of associated second and third mode shapes are insignificant compared with the amplitude of first mode shape ($s = 1$): in this case they do not exceed 2·6% of the first mode shape. At the same time, the amplitudes of associated first and third mode shapes are 12·5 and 13·6% of the second mode shape ($s = 2$), respectively. Note that coefficients P_{ci} ($i \neq s$) depend essentially on the crack location and can in certain cases reach considerable values.

TABLE 1

Geometrical description of the specimens [2, 5, 11, 12]

Material of the specimen	Type of crack	L (mm)	L_c/L	h (mm)	b (mm)	m_L (kg)
Cold rolled steel ATSTC-1018 [5]	Closing	330	0 0·18	25	25	0
Alloy steel 15H2 [11]		184 220	0·01 0·04 0·08 0·14 0·16 0·28	13·8	4	0·234 0·154 0·259 0·154 0·259
Alloy steel 08H18 [11]		150	0·2	20	4	3·520
Steel [12]		300	0·47	20	20	0
Steel [2]	Open	200	0·2 0·55 0·7	7·8	25	0
Titanium alloy VT-8 [11]		220	0·09 0·18 0·52	20	4	0·150 0·255

Thus, if the analysis of the first cycle of vibration shows that the amplitudes of associated mode shapes are insignificant (as it takes place for the above-mentioned specimens at $s = 1$) then the solution for the second half-cycle (28) can be simplified to the form

$$y_{cj}(x, t) = P_{cs} w_{sj}(x) \sin \omega_{os} t. \tag{29}$$

The natural frequency of the sth mode shape of the beam with a closing crack may be calculated by the following formula [30]

$$\omega_{cs} = \frac{2\omega_s \omega_{os}}{(\omega_s + \omega_{os})}. \tag{30}$$

A closing crack causes the distortion of harmonicity of time functions describing the vibration characteristics of the cracked beam. To determine the distortion of the wave shape of displacement, strain or acceleration of different cross-sections of the beam by the higher harmonics method [20, 21] it is necessary to establish equations which connect this wave shape to crack parameters. From equations (24) and (29) which describe the wave shape of displacement it is not difficult to derive the expression for the wave shape of acceleration for different half-cycles of vibration:

$$\frac{\partial y^2(x, t)}{\partial t^2} = -\omega_s^2 w_s(x) \sin \omega_s t, \tag{31}$$

$$\frac{\partial y_{cj}^2(x, t)}{\partial t^2} = -\omega_{os}^2 P_{cs} w_{sj}(x) \sin \omega_{os} t. \tag{32}$$

For different half-cycles of vibration while the crack is closed and open the normalized distribution function of strain along the beam length can be represented, respectively,

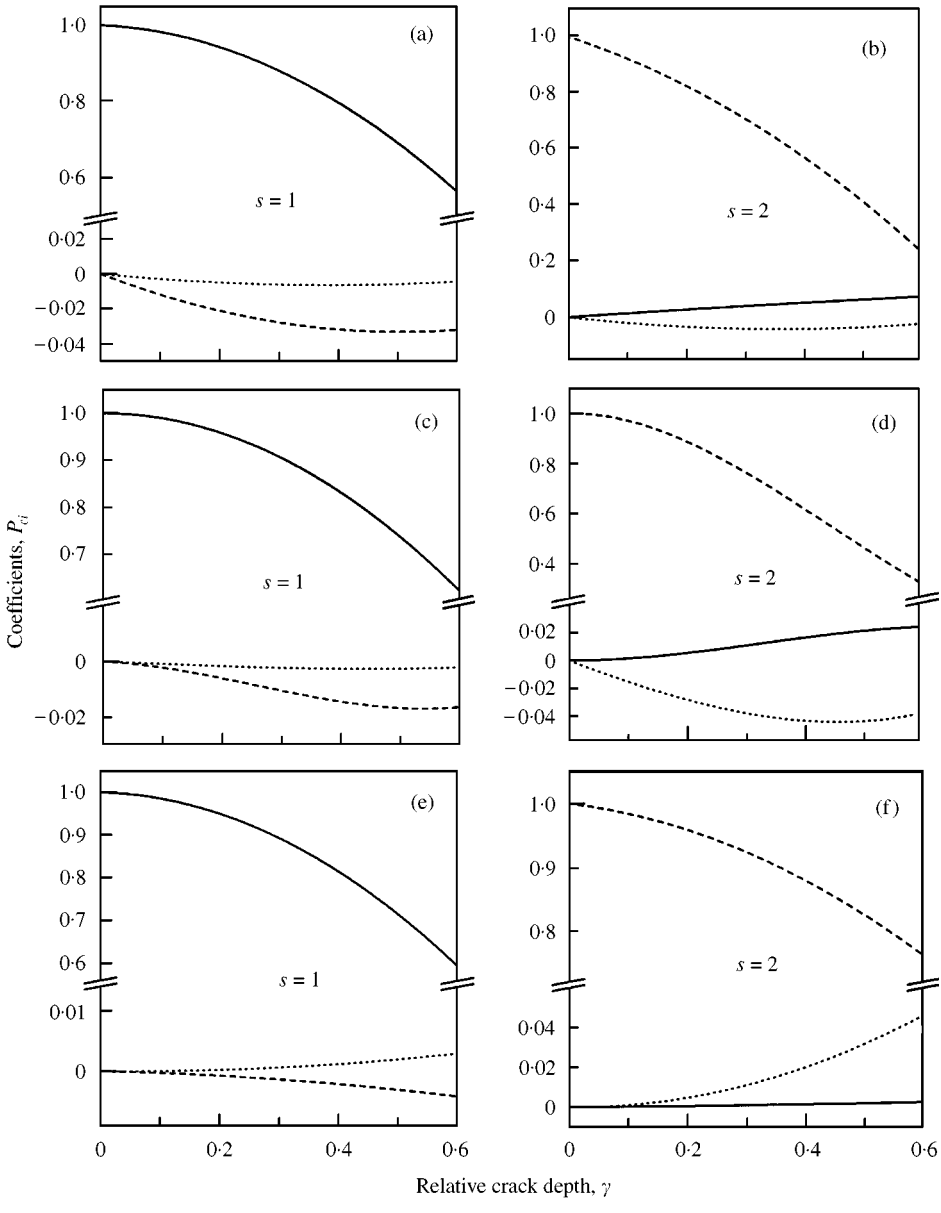

Figure 2. Relative crack depth dependence of the coefficients P_{ci} for the steel ATSTC-1018 ($L_c/L = 0$) (a)–(b), steel 15H2 ($L = 0{\cdot}184$ mm) (c)–(d), and steel 08H18 (e)–(f); ——, $i = 1$; – – – –, $i = 2$ ·····, $i = 3$.

in the form

$$\bar{\varepsilon}(x, t) = \bar{M}_s(x)\sin \omega_s t, \tag{33}$$

$$\bar{\varepsilon}_c(x, t) = f_\varepsilon(x, \gamma)P_{cs}\bar{M}_{sj}(x)\sin \omega_{os} t, \tag{34}$$

where function $f_\varepsilon(x, \gamma)$ takes into account the effect of the crack on the strain distribution, and $\bar{M}_s(x)$ and $\bar{M}_{ij}(x)$ are the normalized distribution function of the bending moment along the length of crack-free and cracked beam, respectively ($\bar{M}_s(0) = \bar{M}_{ij}(0) = 1$).

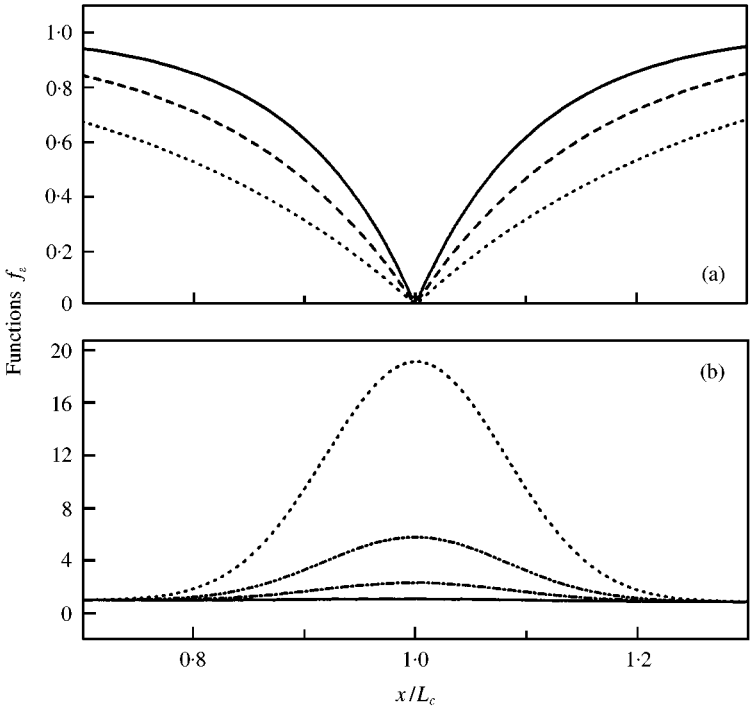

Figure 3. Strain distributions in the vicinity of crack on the cracked (a) and uncracked (b) surface of beam ($h = 13{\cdot}8$ mm); ——, $\gamma = 0{\cdot}1$, – – –, $\gamma = 0{\cdot}2$; – · –, $\gamma = 0.4$; – · · – · · –, $\gamma = 0.6$; · · · · · ·, $\gamma = 0{\cdot}8$.

On the cracked surface of the beam, the function $f_\varepsilon(x, \gamma)$ can be represented in the form

$$f_\varepsilon(x, \gamma) = 1 - \exp\left(- \frac{2\alpha(\gamma)|x - L_c|}{h} \right), \tag{35}$$

where $\alpha(\gamma) = 0{\cdot}683 + 0{\cdot}152/\gamma$ (at $\gamma = 0$ it is accepted that $f_\varepsilon(x, \gamma) = 1$). Equation (35) is a result of some modification of the expressions used by Shen and Pierre [16] for the description of stress and strain distribution along the length of cracked beam (it was accepted in reference [16] that $\alpha = 1{\cdot}276$). Finite-element analysis of strain distribution in the vicinity of the crack enabled determination of the crack depth dependence of this distribution (Figure 3(a)) and to obtain the function of strain distribution on the surface opposite to the cracked surface of the beam (Figure 3(b)):

$$f_\varepsilon(x, \gamma) = 1 + [\beta(\gamma) - 1]\exp\left[- \left(\frac{L_c - x}{\upsilon(\gamma)h} \right)^2 \ln \beta(\gamma) \right], \tag{36}$$

where $\beta(\gamma) = 0{\cdot}123 + 0{\cdot}813\exp(\gamma) + 0{\cdot}064\exp(7\gamma)$, $\upsilon(\gamma) = 0{\cdot}063 + 0{\cdot}45\gamma$.

As can be seen from Figure 3, the intensity functions $f_\varepsilon(x, \gamma)$ in the vicinity of the crack are important. Therefore, for strain measurements by strain guages, the location of the strain guages as well as their base will affect the strain wave shape. Averaged over the strain guage

base, strain wave shapes are determined for the crack-free and cracked beam by the following expressions respectively:

$$\bar{S}(L_B, B) = \frac{1}{B} \sin \omega_s t \int_{B_1}^{B_2} M_s(x)\, dx, \tag{37}$$

$$\bar{S}_{cj}(L_B, B) = \frac{1}{B} P_{cs} \sin \omega_{os} t \int_{B_1}^{B_2} f_\varepsilon(x, \gamma) \bar{M}_{sj}(x)\, dx, \tag{38}$$

where L_B and B are the strain guage location and base (see Figure 1), $B_1 = L_B - B/2$, $B_2 = L_B + B/2$.

Thus, the cracked beam model enables the relationships of natural frequencies and mode shapes with respect to crack depth and location in the case of open or closing edge transverse cracks to be derived. In addition, the above expressions for the wave shapes of displacement, acceleration and strain make it possible to investigate the higher harmonics in the Fourier-series expansion of those expressions for the beam with a closing crack in the case of the negligible amplitudes of associated mode shapes:

$$F_c(x, t) = \frac{a_0}{2} + \sum_{n=1}^{\infty} (a_n \cos n\omega_{cs} t + b_n \sin n\omega_{cs} t), \tag{39}$$

where

$$a_n = \frac{\omega_{cs}}{\pi} \left[\int_{-\pi/\omega_s}^{0} f(x, t) \cos n\omega_{cs} t\, dt + \int_{0}^{\pi/\omega_{os}} f_c(x, t) \cos n\omega_{cs} t\, dt \right], \quad n = 0, 1, 2, \ldots, \tag{40}$$

$$b_n = \frac{\omega_{cs}}{\pi} \left[\int_{-\pi/\omega_s}^{0} f(x, t) \sin n\omega_{cs} t\, dt + \int_{0}^{\pi/\omega_{os}} f_c(x, t) \sin n\omega_{cs} t\, dt \right], \quad n = 0, 1, 2, 3, \ldots. \tag{41}$$

For the displacement, the wave shape functions $f(x, t)$ and $f_c(x, t)$ are determined by equations (24) and (29) respectively; for the acceleration wave shape by equations (31) and (32); for the strain wave shape by equations (33) and (34); and for the strain wave shape from a strain guage by equations (37) and (38).

4. ESTIMATION OF VALIDITY OF THE ANALYTICAL APPROACH

The estimation of the validity of the analytical approach was carried out based on the comparison of the results of calculations with the results of laboratory tests of the specimens with fatigue [5, 11] and open [2, 11] cracks. The geometrical characteristics of the specimens are shown in Table 1.

The results for certain specimens with fatigue (closing) crack are presented in Table 2. As can be seen, the experimental and predicted values of the relative change of the first natural frequency are very close. Analysis of the results for the alloy steel 15H2 specimens ($L = 220$ mm) showed that at $\gamma \leqslant 0{\cdot}5$ the difference between the results of experimental and

TABLE 2

Experimental and predicted magnitudes of the relative change of first natural frequency and crack depths for the specimens with fatigue (closing) crack

Specimen	L_c/L	γ	f_a/f		Δ_f (%)	a (mm)		Δ_a (%)
			Experiment	Predicted		Experiment	Predicted	
ATSTC-1018 [5]	0	0·2	0·924	0·969	− 4·8	5	7·8	− 56·0
		0·4	0·871	0·873	− 0·2	10	10·1	− 1·0
		0·6	0·725	0·704	2·9	15	14·5	3·3
	0·18	0·2	0·947	0·983	− 3·8	5	8·6	− 72·0
		0·4	0·901	0·926	− 2·8	10	11·3	− 13·0
		0·6	0·830	0·802	3·4	15	14·2	5·3
15H2 [11]	0·01	0·18	0·984	0·985	− 0·1	2·5	2·6	− 4·0
		0·36	0·942	0·944	− 0·2	4·9	5·0	− 2·0
		0·46	0·911	0·901	1·1	6·3	6·0	4·8
		0·51	0·884	0·872	1·4	7·0	6·7	4·3
		0·60	0·797	0·797	0	8·3	8·3	0
		0·72	0·655	0·654	0·2	9·9	9·9	0
08H18 [11]	0·2	0·1	0·979	0·995	− 1·6	1·9	3·7	− 94·7
		0·2	0·960	0·976	− 1·7	4·0	5·1	− 27·5
		0·31	0·943	0·943	0	6·1	6·1	0
		0·39	0·913	0·903	1·1	7·8	7·4	5·1
		0·51	0·845	0·830	1·8	10·1	9·7	4·0
		0·6	0·765	0·749	2·1	12·0	11·7	2·5

analytical determination of the relative change of first natural frequency was in the range $-6{\cdot}4 \leqslant \Delta_f \leqslant 2{\cdot}1\%$. At $\gamma > 0{\cdot}5$ this difference was up to $-37{\cdot}8\%$. In all likelihood, in the case of a large crack it is practically impossible to avoid plastic strains in the cross-section weakened by a crack and as a result a closing crack becomes an open one in part or entirely. Indirectly, this assumption is corroborated by the results of calculations for the alloy steel 15H2 specimens when the crack is open: in this case, the maximal distinction between the results of experiment and calculation at $\gamma > 0{\cdot}5$ did not exceed 8·3%.

It is obvious that the choice of the expression for the stress intensity factor will influence the equivalent stiffness of the cross-section with crack and, consequently, the natural frequencies and mode shapes. These investigations showed that expression (18) from Cherepanov [29] gives the best agreement between the results of experiment and calculation of the natural frequency of the specimens with a closing and with an open crack. For an open crack the comparison was conducted based on the results of experiments reported in references [2, 11] (see Table 3).

As seen in Table 3, the distinction between the experimental and predicted results of the relative change of natural frequencies is even less than in the case of a closing crack, with the exception of two results for the alloy VT-8 specimen ($L_c/L = 0{\cdot}52$, $\gamma = 0{\cdot}6$ and 0·8). Note that the difference between the results of calculations executed by Shen and Pierre [16] with a local Ritz method and the results of experiment conducted by Wendtland [2] was somewhat greater (except the third mode o vibration): in the range $-1{\cdot}2 \leqslant \Delta_f \leqslant 11{\cdot}9\%$ for the first mode, $-2{\cdot}1 \leqslant \Delta_f \leqslant 6{\cdot}6\%$ for the second mode, and $-1{\cdot}1 \leqslant \Delta_f \leqslant 1{\cdot}0\%$ for the third mode of vibration for a relative crack depth $0.13 \leqslant \gamma \leqslant 0.8$.

The present analytical approach enables one to solve the inverse problem of damage diagnostics. Thus, based on the results of measurements of resonance frequencies of the

TABLE 3

Experimental and predicted magnitudes of the relative change of natural frequencies and crack depths for the specimens with open crack

Specimen	s	L_c/L	γ	f_a/f		Δ_f (%)	a (mm)		Δ_a (%)
				Experiment	Predicted		Experiment	Predicted	
Steel [2]	1	0·2	0·13	0·991	0·994	− 0·3	1	1·2	− 20·0
			0·26	0·974	0·973	0·1	2	2·0	0
			0·4	0·933	0·929	0·4	3·1	3·0	3·2
			0·6	0·812	0·794	2·2	4·7	4·6	3·3
			0·8	0·522	0·520	0·4	6·2	6·2	0
	2	0·55	0·13	0·991	0·994	− 0·3	1	1·2	− 20·0
			0·26	0·978	0·974	0·4	2	1·9	5·0
			0·4	0·933	0·931	0·2	3·1	3·1	0
			0·6	0·805	0·808	− 0·4	4·7	4·7	0
			0·8	0·575	0·588	− 2·3	6·2	6·3	− 1·6
	3	0·7	0·13	0·990	0·993	− 0·3	1	1·2	− 20·0
			0·26	0·972	0·972	0	2	2·0	0
			0·4	0·928	0·928	0	3·1	3·1	0
			0·6	0·833	0·822	1·3	4·7	4·6	2·1
			0·8	0·693	0·698	− 0·7	6·2	6·3	− 1·6
VT-8 [11]	1	0·09	0·1	0·987	0·990	− 0·3	2	2·3	− 15·0
			0·2	0·953	0·960	− 0·7	4	4·3	− 7·5
			0·4	0·830	0·836	− 0·7	8	8·2	− 2·5
			0·6	0·629	0·630	− 0·2	12	12·0	0
			0·8	0·343	0·343	0	16	16·0	0
		0·18	0·1	0·992	0·992	0	2	2·0	0
			0·2	0·967	0·967	0	4	4·0	0
			0·4	0·855	0·860	− 0·6	8	8·2	− 2·5
			0·6	0·676	0·667	1·3	12	11·9	0·8
			0·8	0·385	0·374	2·9	16	15·9	0·6
		0·52	0·2	0·991	0·987	0·4	4	3·3	17·5
			0·4	0·963	0·940	2·4	8	6·5	18·8
			0·6	0·889	0·826	7·1	12	10·2	15·0
			0·8	0·667	0·551	17·4	16	14·7	8·1

specimens with fatigue cracks [5, 11] and with sawing cuts [2, 11] the corresponding values of crack depth were calculated. As seen in Tables 2 and 3, the relative deviation Δ_a of the measured values of crack depth from calculation is inversely proportional to the crack magnitude. Note that the ellipticity of the fatigue crack front was not considered in the calculations. In the experiment [11], the crack depth was measured on the side surfaces of the guage length of the specimen. The investigation of fracture surfaces of the specimens with fatigue cracks showed that the crack's depth in the middle of crack front was 0·2–0·4 mm greater than the crack's depth on the edges of the front. In all likelihood, this fact is one of the reasons that in the range of small cracks the distinction between the results of experiment and calculation is greatest and that calculation gives overestimated values of crack depth. At the same time, the distinction between the results of experiment and calculation for the relative change of natural frequency is lowest in the range of small cracks ($\gamma \leqslant 0{\cdot}5$). This is evident if one compares the corresponding values of Δ_a and Δ_f in Tables 2 and 3. Consequently, high accuracy of analytical determination of the decrease in natural frequency does not always signify the same accuracy of crack magnitude determination. This result confirms the conclusion of the reference [11].

The authors know of only one experimental investigation of natural mode shapes of a cantilever beam with a fatigue crack [12] (see Table 1). The calculation of mode shapes for this beam was executed using expressions (24) and (29) as the mean of values $y(x, -\pi/2\omega_s)$ and $y_{cj}(x, \pi/2\omega_{os})$. The results of experiment and calculation are shown in Figure 4. The analytical approach does not permit complete simulation of the conditions of the test; that is the displacement of the accelerometer along the length of the beam in the process of experimental modal analysis. Additionally, even a relatively small mass placed in different points on the beam will change its mode shapes, especially higher ones. In all likelihood, this

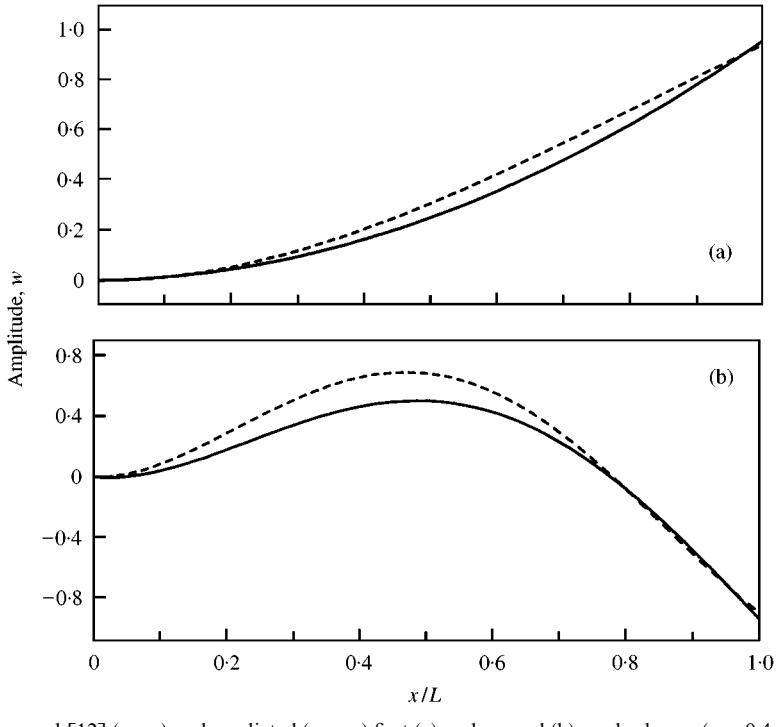

Figure 4. Measured [12] (——) and predicted (– – – –) first (a) and second (b) mode shapes ($\gamma = 0{\cdot}4$, $L_c/L = 0{\cdot}47$).

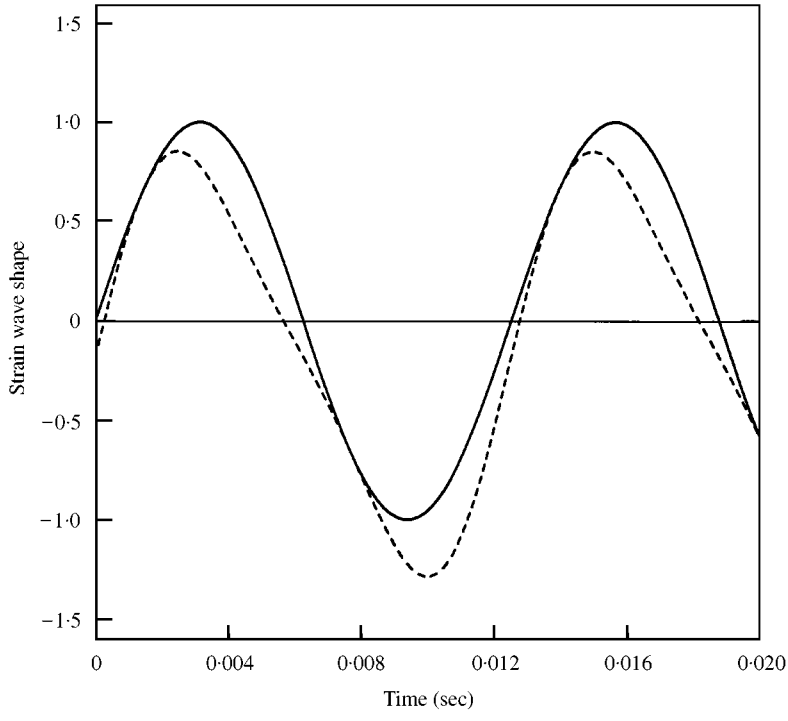

Figure 5. Strain wave shape on the uncracked (——) and cracked (– – – –) surface of the steel 08H18 specimen ($\gamma = 0{\cdot}39$, $L_B/L = 0{\cdot}47$).

circumstance is the chief cause of the somewhat greater difference between the results of the experiment and the calculation for the second mode shape.

As is well known, the presence of a crack distorts the wave shape of any characteristic of vibration of the cracked beam; that is, for example, displacement, velocity, acceleration, strain etc. In Figure 5, the time function of strain ($L_B = 42{\cdot}5$ mm, strain guage glued on the cracked side of the specimen) is shown for the crack-free and cracked steel 08H10 specimen. One can evaluate this distortion by the amplitudes and phases of higher harmonics in the Fourier-series expansion of corresponding time functions.

An experimental procedure for harmonic analysis of stress and strain wave shapes [31] was used for the detection of higher harmonics in the Fourier-series expansion of strain and acceleration wave shapes on tests of the specimens [11] (see Table 1) at the first mode of vibration ($s = 1$). Strain measurements were carried out with foil strain guages ($B = 5$ mm). For the acceleration measurement an accelerometer (Bruel & Kjaer, Type 4370) was attached to the end of the specimens.

As may be seen from Figures 6 and 7, good agreement between the results of experiment and calculation for the amplitude of the second harmonic of the strain wave shape (in Figures 6–9 the amplitudes of higher harmonics are shown relative to the amplitude of the first harmonic b_1).

On the alloy steel 08H18 specimen the strain guage was glued on the surface with the crack and on the alloy steel 15H2 specimens on the opposite from the cracked side surface. In certain cases, the quantitative difference between the results of experiment and calculation was considerable as, for example, for the zero harmonic a_0 (steel 08H18,

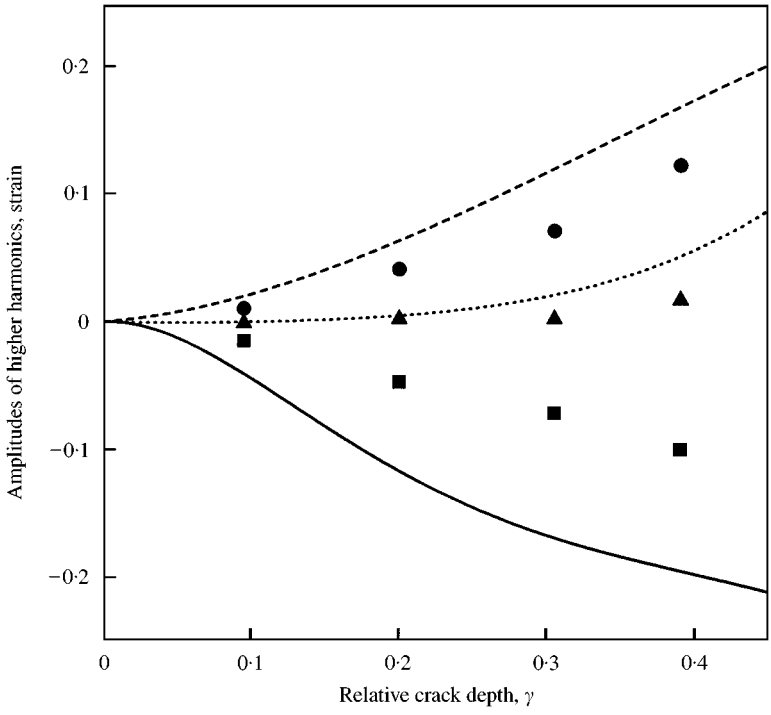

Figure 6. Effect of crack depth on the amplitudes of higher harmonics in strain wave shape on the uncracked side surface of the steel 08H18 specimen ($L_B/L = 0{\cdot}283$); ■, ———, a_0/b_1; ●, – – – –, a_2/b_1; ▲, ·····, b_2/b_1 (symbols—experiment, curves—predicted).

Figure 6). However, it is necessary to emphasize that all analytically predicted relationships describe the results of experiment qualitatively. The illustration of the strain guage location effect ($L_B \pm 1$ mm) on the amplitude of the second harmonic is shown in Figure 7 (this was the simulation of possible error of the value L_B measurement in the experiment). As may be seen, the effect of measurement error of parameter L_B on higher harmonics is small. Analytical investigations showed that this effect decreases abruptly as the strain guage location is moved way from the cross-section with a crack and may be neglected.

An analytical investigation of higher harmonics in the acceleration wave shape also was conducted. As seen in Figures 8 and 9, good qualitative agreement between the results of calculation and experiment is observed for the second harmonics and zero harmonic of the acceleration wave shape. Similar results were obtained for other specimens with a closing crack.

For the specimens with an open crack (alloy VT-8) the results of calculation and experiment are sufficiently close inasmuch as the analytical approach does not show zero and higher harmonics in strain and acceleration wave shape. Experiment also showed that the amplitudes of the harmonics are close to zero (the error of experimental procedure of zero harmonic measurement may be high because of uncontrollable zero drift of amplifiers).

Quantitative differences between the results of calculation of higher harmonics in strain and acceleration wave shapes and corresponding experiment may be connected with the possible effect of damping, impact of crack surfaces, ellipticity of crack front, or measurement error of dynamic characteristics.

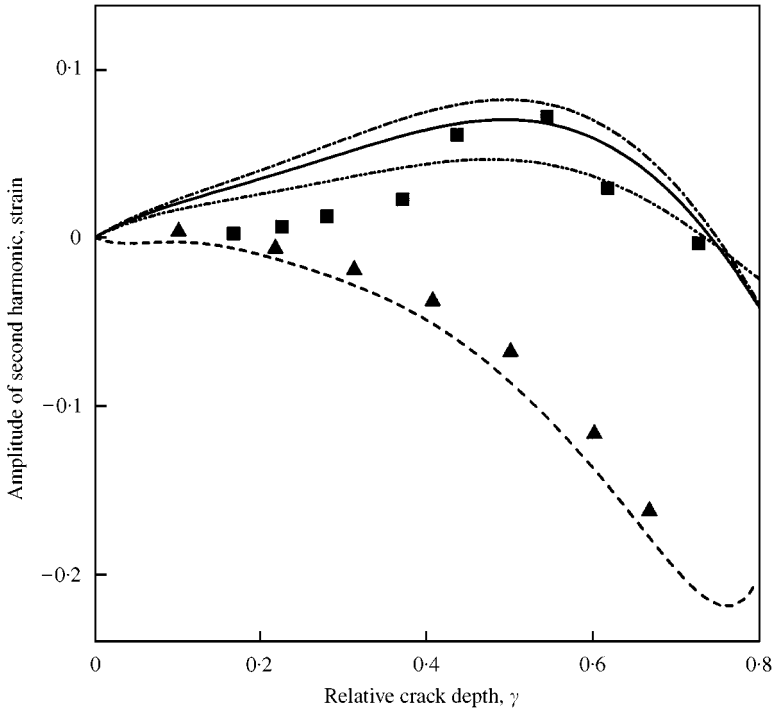

Figure 7. Effect of crack depth on the amplitude of second harmonic a_2/b_1 in strain wave shape on the uncracked side surface of the steel 15H2 specimen ($L = 200$ mm); ■, ———, $L_B = 9{\cdot}5$ mm, –·–·–, $L_B = 8{\cdot}5$ mm, –··–··–, $L_B = 10{\cdot}5$ mm, $L_c/L = 0{\cdot}04$; ▲, $L_B = 10$ mm, $L_c/L = 0{\cdot}28$ (symbols—experiment, curves—predicted).

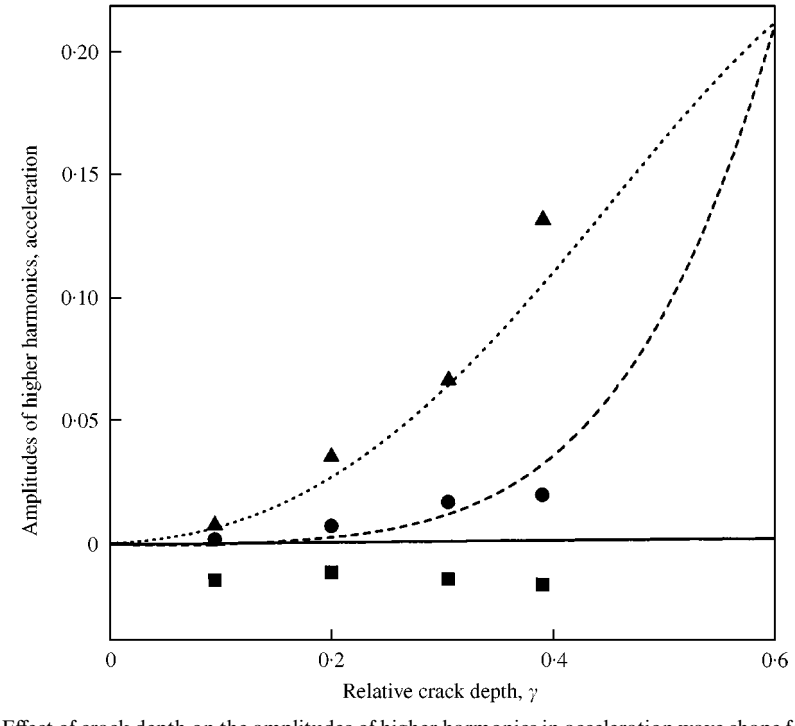

Figure 8. Effect of crack depth on the amplitudes of higher harmonics in acceleration wave shape for the 08H18 specimen; ■, ———, a_0/b_1; ▲, ·····, a_2/b_1; ●, – – – –, b_2/b_1; (symbols—experiment, curves—predicted).

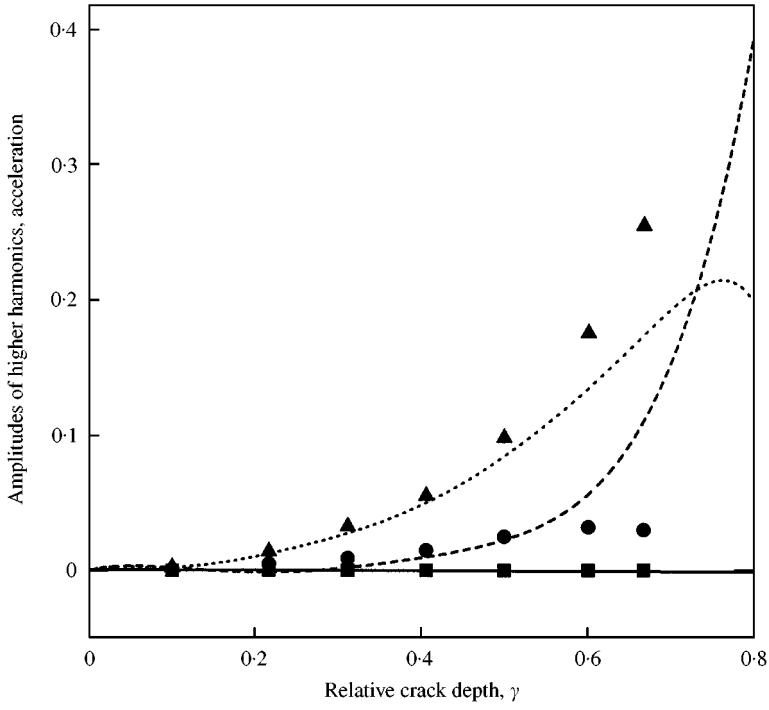

Figure 9. Effect of crack depth on the amplitudes of higher harmonics in acceleration wave shape for the steel 15H2 specimen ($L = 220$ mm, $L_c/L = 0{\cdot}28$); ■, ———, a_0/b_1; ▲, ·····, a_2/b_1; ●, – – – –, b_2/b_1; (symbols—experiment, curves—predicted).

5. CONCLUSIONS

An analytical approach that enables investigation of dynamic characteristics of a beam with a closing (fatigue) crack is developed.

It is shown that in the process of the crack opening the origination of associated mode shapes differing from the initially given mode shape takes place. In the case of the initially given first mode shape ($s = 1$), the amplitudes of higher mode shapes are relatively small. In the case of the initially given second or more higher mode shape, the amplitudes of associated mode shapes under certain conditions can be comparable with the amplitude of the initially given mode shape.

The predicted values of natural frequencies and mode shapes for the specimens with a fatigue crack are close to those obtained experimentally, as well as the results of calculation and experimental estimation of distortion of strain and acceleration wave shapes. The verification of the analytical approach with a considerable amount of experimental data and with the results of other author's calculations showed that the analytical approach enables one to obtain well-founded relationships between different dynamic characteristics and crack parameters and to solve the inverse problem of damage diagnostics with sufficient accuracy for practical purposes.

REFERENCES

1. M. KRAWCZUK and W. OSTACHOWICZ 1996 *Journal of Theoretical and Applied Mechanics* **34**, 307–326. Damage indicators for diagnostic of fatigue cracks in structures by vibration measurements—a survey.

2. D. WENDTLAND 1972 *Ph.D. Thesis, University of Karlsruhe*, Änderung der biegeeigenfrequenzen einer idealisierten Schaufel durch Risse.
3. P. GUDMUNDSON 1982 *Journal of the Mechanics and Physics of Solids* **30**, 339–353. Eigenfrequency changes of structures due to cracks, notches or other geometrical changes.
4. P. GUDMUNDSON 1983 *Journal of the Mechanics and Physics of Solids* **31**, 329–345. The dynamic behaviour of slender structures with cross-sectional cracks.
5. A. IBRAHIM, F. ISMAIL and H. K. MARTIN 1990 *Journal of Sound and Vibration* **140**, 305–317. Identification of fatigue cracks from vibrating testing.
6. G.-L. QIAN, S.-N. GU and J.-S. JIANG 1990 *Journal of Sound and Vibration* **138**, 233–243. The dynamic behaviour and crack detection of a beam with a crack.
7. A. JOSHI and B. S. MADHUSUDHAN 1991 *Journal of Sound and Vibration* **147**, 475–488. A unified approach to free vibration of locally damaged beams having various homogeneous boundary conditions.
8. W. M. OSTACHOWICH and M. KRAWCZUK 1991 *Journal of Sound and Vibration* **150**, 191–201. Analysis of the effect of cracks on the natural frequencies of a cantilever beam.
9. M. L. KIKIDIS and C. A. PAPADOPOULOS 1992 *Journal of Sound and Vibration* **155**, 1–11. Slenderness ratio effect on cracked beams.
10. A. RYTTER, R. BRINCKER and P. H. KIRKEGAARD 1992 *Fracture & Dynamics, Paper No.* 37, *Department of Building Technology and Structural Engineering, University of Aalborg*. An experimental study of the modal parameters of a damaged cantilever.
11. A. P. BOVSUNOVSKY 1999 *Strength of Materials* **31**, 45–53. To the question on determination of transverse and axial natural frequency of vibration of a cracked beam. Part 2. Results of experiment and calculation.
12. P. F. RIZOS, N. ASPRAGATHOS and A. D. DIMAROGONAS 1990 *Journal of Sound and Vibration* **138**, 381–388. Identification of crack location and magnitude in a cantilever beam from the vibration modes.
13. K. D. HJELMSTAD and S. SHIN 1996 *Journal of Sound and Vibration* **198**, 527–545. Crack identification in a cantilever beam from modal response.
14. P. G. KIRSHMER 1994 *Proceedings of ASTM*, Vol. **44**, 897–904. The effect of discontinuities on the natural frequency of beams.
15. W. T. THOMSON 1949 *Journal of Applied Mechanics* **16**, 203–207. Vibration of slender bars with discontinuities in stiffness.
16. M.-H. H. SHEN and C. PIERRE 1994 *Journal of Sound and Vibration* **170**, 237–259. Free vibrations of beams with a single-edge crack.
17. V. P. GOLUB, V. P. BUTSEROGA and A. D. POGREBNIAK 1995 *International Applied Mechanics* **31**, 66–74. Investigation of kinetics of fatigue cracks by differential compliance method.
18. N. P. PLAHTIENKO and S. A. YASINSKIY 1995 *Strength of Materials* **27**, 146–152. Resonance of second order in vibrations of a beam containing a transverse crack.
19. T. J. ROYSTON and R. SINGH 1996 *Journal of Sound and Vibration* **198**, 279–298. Experimental study of a mechanical system containing a local continuos stiffness non-linearity under periodic excitation and static load.
20. V. V. MATVEEV 1997 *Strength of Materials* **29**, 561–572. Efficiency of method of spectral vibrodiagnostics for fatigue damage of structural elements. Part 1. Longitudinal vibrations, analytical solution.
21. V. V. MATVEEV and A. P. BOVSUNOVSKY 1998 *Strength of Materials* **30**, 564–574. Efficiency of the method of spectral vibrodiagnostics for fatigue damage of structural elements. Part 2. Bending vibrations, analytical solution.
22. A. B. ROITMAN, A. A. PYLOV and N. B. ALEKSANDROVA 1999 *Strength of Materials* **31**, 23–34. Axial vibrations of cantilever beam with transverse crack. Part 1. Small vibrations.
23. R. D. ADAMS, P. CAWLEY, C. J. PYE and B. J. STONE 1978 *Journal of Mechanical Engineering Science* **20**, 93–100. A vibration terchnique for non-destructively assessing the integrity of structures.
24. H. J. PETROSKI 1981 *International Journal of Fracture* **17**, R71–R76. Simple static and dynamic models for the cracked elastic beam.
25. S. CHRISTIDES and A. D. S. BARR 1984 *International Journal of Mechanical Sciences* **26**, 639–648. One-dimensional theory of cracked Bernouly–Euler beams.
26. M. CHATI, R. RAND and S. MUKHERJEE 1997 *Journal of Sound and Vibration* **207**, 249–270. Modal analysis of a cracked beam.
27. Y. G. PANOVKO 1957 *Fundamentals of Applied Theory of Elastic Vibrations*. Moscow: Machine-building literature (in Russian).

28. H. TADA, P. PARIS and G. IRWIN 1973 *The Stress Analysis of Crack Handbook*. Hellertown, Pensilvania: Del Research Corporation.
29. G. P. CHEREPANOV 1974 *Mechanics of Brittle Fracture*. Moscow: Nauka (in Russian).
30. S. TIMOSHENKO, D. H. YOUNG and W. WEAVER Jr 1974 *Vibration Problems in Engineering*. New York: Wiley, fourth edition.
31. A. P. BOVSUNOVSKY and A. G. KRATKO 1998 *Journal of Testing and Evaluation* **26**, 31–37. The shape of mechanical hysteresis loops for metals under harmonic loading.

APPENDIX A: NOMENCLATURE

a	crack depth
A	beam cross-sectional area
b	width of cross-section
B	base of strain guage
d	parameter to be determined
E	Young's modulus
f	resonance frequency of crack-free specimen
f_a	resonance frequency of cracked specimen
h	height of cross-section
i	number of mode shape
I	crack-free cross-sectional area moment of inertia
I_m	end mass moment of inertia
I_o	cracked cross-sectional area moment of inertia
$K_I(a)$	stress intensity factor
L	length of beam
L_c	co-ordinate of the cross-section with crack
L_B	location of strain guage
m	beam mass per unit length
m_L	end mass
$M(x)$	bending moment
$Q(x)$	transverse force
s	initially given mode shape
S	Krylov function
T	Krylov function
U	Krylov function
V	Krylov function
$v(x)$	velocity
$w(x)$	mode shape of a beam
$y(x)$	displacement
Δ_a	relative distinction between the results of experiment and calculation of the crack depth
Δ_f	relative distinction between the results of experiment and calculation of the relative change of natural frequency
γ	relative crack depth
$\theta(x)$	angle of rotation
ρ	density
ω	natural frequency of the crack-free beam
ω_o	natural frequency of the beam with open crack
ω_c	natural frequency of the beam with closing crack